An NMR Spectroscopy and Molecular Mechanics Study of the Molecular Basis for the Supramolecular Structure of Lipopolysaccharides†

Ying Wang‡ and Rawle I. Hollingsworth*,‡,§

Departments of Chemistry and Biochemistry, Michigan State University, East Lansing, Michigan 48824-1319

Received March 22, 1995; Revised Manuscript Received November 13, 1995⊗

ABSTRACT: Lipopolysaccharides from Gram-negative bacteria interact with the mammalian immune system to trigger a cascade of physiological events leading to a shock syndrome which results in death in over 70% of cases of severe shock. It is known that the supramolecular structures of lipopolysaccharide aggregates are critical contributors to their biological activities. Despite this, the molecular basis for the formation of the regular hexagonal plates and arrays observed in lipopolysaccharide films and suspensions is unknown. Since these structures are two dimensional, it is unlikely that X-ray crystallographic methods will shed much light on their detailed structure. Knowing this structure is important since it is becoming increasingly likely that insertion of the lipopolysaccharide hydrocarbon chains into the target host cell membrane may be involved in triggering host responses. This work describes the three-dimensional structure of the lipopolysaccharide lipid A moiety. The structure was obtained by a combination of molecular mechanics calculations and nuclear magnetic resonance spectroscopy. This involved calculation of the dihedral angle between the two glucosamine residues of the lipid A molecule from coupling constants and measuring critical interresidue NOE values. The study also takes into account information from X-ray powder diffraction and electron microscopy studies.

Lipopolysaccharides (LPSs)[1] are complex lipid-linked carbohydrates which are found in the outer membranes of Gram-negative bacteria. These molecules are usually composed of a polymeric carbohydrate region called the O-antigen, a short oligosaccharide region called the R-core, and a fatty-acylated region (usually a glucosamine disaccharide) called the lipid A (Rietschel et al., 1990). The lipid A molecule is usually bisphosphorylated and, in the case of *Escherichia coli* and most bacteria, has the structure shown in Figure 1.

Lipopolysaccharides are potent potentiators of host immune responses in mammalian systems. These responses include the production of interleukins, tumor necrosis factor, and prostaglandins at the cellular level (Gery & Waksman, 1972; Turner et al., 1989; Morrison & Ryan, 1979) and fever, shock, and death at the level of the organism (Schechmeister et al., 1952; Nowotny, 1969). Despite evidence for an interaction between lipopolysaccharides and host immune cells via receptor-mediated pathways involving the carbohydrate headgroup (Raetz, 1993), it is becoming increasingly clear that the supramolecular structure and the fatty acid arrangement of lipopolysaccharides are critical. Several workers have demonstrated a dramatic change in host-cell membrane properties when treated with lipopolysaccharides by a variety of techniques including fluorescence depolarization and electron spin resonance (Price & Jacobs, 1986; Larson et al., 1985; Jackson et al., 1989). It has also been demonstrated that when lipopolysaccharides bind to macrophages, they do so by membrane insertion with the polar, carbohydrate regions facing away from the cell (Jackson et al., 1992). Lipopolysaccharides which lack even one fatty acid group are not toxic (Myers et al., 1990). The biological activity of lipopolysaccharides is affected by their salt forms (Galanos & Lüderitz, 1984). In addition, cationic amphiphilic molecules that are designed to break up the supramolecular structure of lipopolysaccharides cause com-

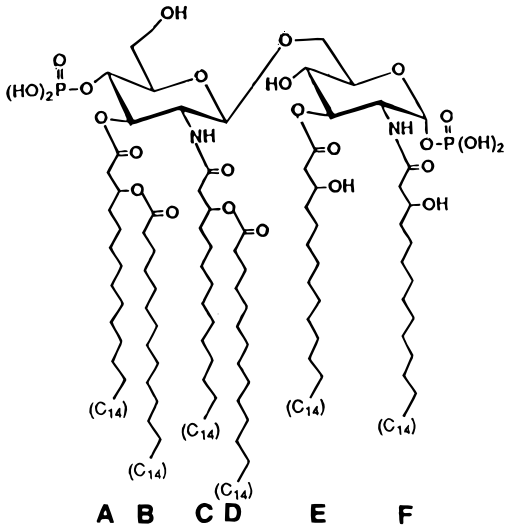

FIGURE 1: Structure of lipid A such as is found in *E. coli* strains. The disaccharide backbone is a β-1,6-linked D-glucosamine disaccharide. 3-Hydroxytetradecanoyl residues are attached to the 2, 3, 2′, and 3′ positions. The fatty acids at the latter two positions are esterified by C-12 and C-14 fatty acids, respectively.

† This work was supported by Grant DE-FG02-89ER14029 to R.I.H. from the U.S. Department of Energy. The NMR data were obtained with instrumentation that was purchased with funds from NIH Grant 1-S10-RR04750, NSF Grant CHE-88-00770, and NSF Grant CHE-92-13241.

* To whom correspondence should be addressed at the Department of Chemistry. Phone, 517-353-0613; Fax, 517-353-9334; E-mail, rih@argus.cem.msu.edu.

‡ Department of Chemistry.

§ Department of Biochemistry.

⊗ Abstract published in *Advance ACS Abstracts,* March 1, 1996.

[1] Abbreviations: DQF-COSY, double-quantum-filtered correlation spectroscopy; HMQC, heteronuclear multiple-quantum coherence; LPS, lipopolysaccharide; NOE, nuclear Overhauser effect; TOCSY, total correlated spectroscopy.

S0006-2960(95)00645-3 CCC: $12.00

plete loss of their biological activity as measured by the *Limulus* amoebocyte lysis assay (Kim et al., 1994). These facts indicate that the supramolecular architectures (geometry and alkyl chain packing) of these molecules are critical determinants of their biological activity and that this activity might be mediated by some bulk colligative property of the lipopolysaccharide in which the fatty acid chain packing plays a critical role. It is, therefore, important to determine how this supramolecular structure may arise. The lipid A moiety is the anchor and structural basement of lipopolysaccharides. It also has the full spectrum of biological properties displayed by the intact LPS molecule. Any regularity in LPS structure must arise from lipid A organization.

Several workers have demonstrated, using electron microscopy, that lipopolysaccharides form structures such as ribbons and sheets in solution (Shands et al., 1967; Shands, 1971). Analysis of transmission electron micrographs of films prepared from such solutions containing calcium or magnesium ions shows that the area of electron density forms a highly ordered hexagonal array mandating that the individual lipopolysaccharide molecules must form structures with a regular geometry. X-ray powder diffraction analyses of hydrated lipopolysaccharides (Kastowsky et al., 1993) show maxima indicating a hexagonal array of lipid molecules. Our studies (data not shown) using X-ray powder diffraction also support this and, in addition, show that lyophilized lipopolysaccharides are microcrystalline and indicate that the hydrocarbon chains are hexagonally packed. Recently, various lipopolysaccharides with lipid A structures similar to that shown in Figure 1 were crystallized and found to form perfectly hexagonal plates (Kato, 1993). However, it is still not known how this might be possible given the structure of the lipid A molecule (Figure 1).

MATERIALS AND METHODS

Diphosphoryl *E. coli* lipid A and Re lipopolysaccharide were purchased from List Biochemicals (Campbell, CA). X-ray powder diffraction analyses were carried out on a RIGAKU diffractometer using a copper source. The K_β line was filtered out. For electron micrographs, a film of *E. coli* Re lipopolysaccharide was formed by spreading a 2% solution of lipopolysaccharide in 0.1 M calcium chloride or magnesium chloride onto carbon-coated grids. Samples were analyzed in transmission mode. Contrast was improved by computer enhancement. NMR spectroscopy was carried out on a Varian VXR500 NMR spectrometer operating at 500 MHz for protons. For NMR spectroscopy, samples were dissolved in a solvent system containing pyridine, 37% deuterium chloride in deuterium oxide, methanol, and chloroform in the ratio of 1:1:2:10, respectively (Wang & Hollingsworth, 1995). All solvents were perdeuterated. Spectra were acquired with a probe temperature of 30 °C. The residual chloroform line at 7.24 ppm was used as a reference. Under these conditions, the residual methanol line appeared at 3.40 ppm. DQF-COSY spectra (Earnst et al., 1987) were acquired for a total of 256 data sets with 32 transients at 2048 data points. Data for the TOCSY experiment (Bax & Davis, 1985) were obtained using similar acquisition conditions. A mixing time of 80 ms was employed. Proton/phosphorus HMQC experiments (Bax & Subramanian, 1986) were performed using a spectral width of 1960 Hz in the phosphorus dimension. A total of 256 data sets were obtained at 24 transients each. For NOE measurements, 256 data sets were also collected with 16 acquisition transients each. Mixing times of 100, 150, 200, and 300 ms were used. Generally, spectra were processed by multiplying the FIDs with a Gaussian function in the f_2 dimension and a shifted Gaussian in f_1. The DQF-COSY spectrum was symmetrized by triangular folding. Molecular mechanics calculations were performed on a Silicon Graphics 4D310 computer using the MM2 (Liljefors et al., 1987) or DREIDING (Mayo et al., 1990) force fields implemented in the BIOGRAF (Molecular Simulations Inc., Waltham, MA 02154) program. The full potential energy functions were used. For the MM2 force field this included a cubic bond stretching potential term, the standard MM2-type valence angle deformation term, a cosine expansion torsional term, an exponential-6 van der Waals potential term, and the usual Coulombic potential for evaluating electrostatic energy. There were no inversion nor hydrogen-bonding terms in the force field. The Dreiding force field included a harmonic term for the bond distortions, a simple harmonic function for the valence angle term, an improper torsion term to evaluate inversions about atomic centers, a Lennard-Jones 12-6 potential for van der Walls contributions, and a Lennard-Jones 12-10 potential for evaluating hydrogen-bonding contributions. The terms used for evaluating torsional and electrostatic contributions were similar to those used in the MM2 method. Charges were calculated using the method of Gasteiger and Marsili (1980). A charge of 1.5 (consistent with accepted levels of ionization under biological conditions) was assigned to each phosphate group. This was divided equally between the three monosubstituted oxygen atoms of the phosphate groups. Calcium ions were assigned a charge of +2. A dielectric of 60−80 (values in that range gave essentially the same results) typical for aqueous systems was used under the assumption that the headgroup region would be reasonably well solvated. Interactions were summed over a 12 Å cutoff. Minimizations were performed using the conjugate gradient method. Simulated annealed dynamics was used to avoid local minima. The MM2 and DREIDING force fields are both well parametrized for hydrocarbons. The default parameters given in the program for the carbohydrate rings were used without modification. This was reasonable since any unusual conformations of the carbohydrate rings could be checked independently by the NMR experiments. Any unusual flattening or puckering of the carbohydrate rings should result in predictable changes in the chemical shifts and coupling constants of the ring protons. This information could then be used as constraints if necessary.

RESULTS AND DISCUSSION

An electron micrograph of a dried film of rough (Re) lipopolysaccharide from *E. coli* is shown in Figure 2. The hexagonal order is readily observable. This agrees well with results obtained by other workers (Shands et al., 1967; Shands, 1971; Kato, 1993). Because lipopolysaccharides self-assemble so readily to form such highly ordered structures, they must exhibit a high degree of symmetry at the molecular level. Molecular mechanics calculations, aided by interactive graphics provided by the BIOGRAF program, were performed in order to arrive at possible symmetrical structures for a bisphosphorylated lipid A molecule bearing six fatty acid chains. Specific structural requirements had to be met for any proposed structure. The six fatty acid

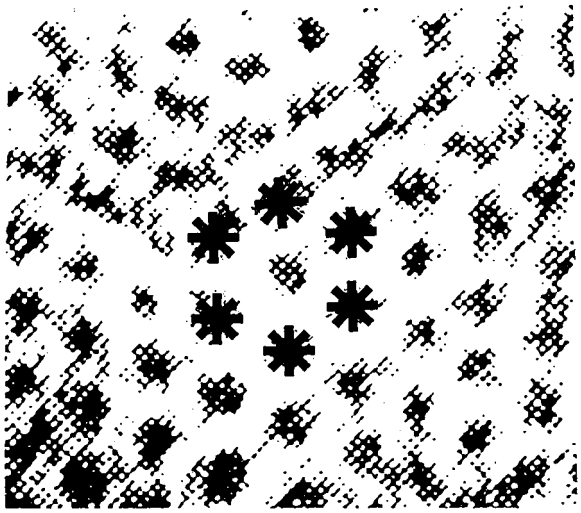

FIGURE 2: Electron micrograph of a dried film of rough (Re) lipopolysaccharide. Note the hexagonal array.

chains must be arranged so as to form the most densely packed system since the hexagonal array is the most densely packed array. Such an arrangement of six parallel hydrocarbon chains would have a triangular cross section perpendicular to their long axis. The sides of such a triangle are all equal in length. This would also give a maximum value for the van der Waals energy of interaction of the extended alkyl chains. An equilateral triangle is also the fundamental regular geometric unit of a regular hexagon.

The disaccharide headgroup conformation (assuming no departure from the regular chair geometry of the pyranose rings) which allowed this fatty acid arrangement was one in which the planes of the two carbohydrate rings were at right angles. In this arrangement, the phosphate groups are at a maximum separation and symmetrically displaced relative to the triangular cross section of the hydrocarbon chains (Figure 3). This conformation was also attractive because it corresponded to a favorable torsional interaction term (global minimum) about the interglycosidic bond. This latter fact was ascertained by evaluating the interaction energies about the interglycosidic angles ϕ (O-5′−C-1′−O-1′−C-6) and ψ (C-1′−O-1′−C-6−C-5) in a Monte Carlo search. Such an arrangement immediately imposed some mandatory structural requirements which could be substantiated by NMR spectroscopy and which, once substantiated, would verify the model. The first of these requirements was that carbohydrate rings should remain in the $^4C_1$ configuration. This could readily be ascertained by evaluating the coupling constants of the anomeric protons and other ring protons. The second aspect that could be validated by NMR spectroscopy was the distances between the anomeric proton of the distal glucosamine ring and the C-4, C-6R, and C-6S protons of the proximal ring. From the molecular model, these distances were 2.28, 2.59, and 3.63 Å, respectively, and represented the only possible inter-ring proton−proton interaction which could give rise to a substantial nuclear Overhouser effect (NOE) in NMR spectroscopy. The third condition was the dihedral angle (ω) about the bond between C-5 and C-6 of the proximal glucosamine ring. The measured value for this from the model was −53.06°. The values for ϕ and ψ obtained from the model were −75.42° and −96.94°, respectively. An analysis of the conformational space about the interglycosidic bond also indicated

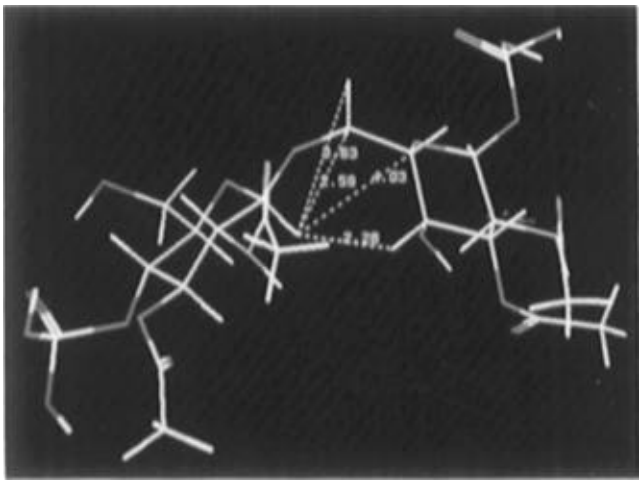

FIGURE 3: Computer model of the bisphorphorylated glucosamine headgroup of the lipid A molecule as it is proposed to be present in the intact structure. The N-linked fatty acids in lipid A have been replaced by *N*-acetyl groups. Note that the planes of the two glycosyl rings are orthogonal. The separations between H-1′ (the anomeric proton of the distal glucosamine ring) and H-4, H-5, H-6R, and H-6S of the proximal ring are indicated. These are 2.28, 4.03, 2.59, and 3.63 Å, respectively (the proximal ring is indicated). The values of the torsion angles (ϕ, ψ, and ω) about the interglycosidic and the C-5−C-6 bonds are −75.42°, −96.94°, and −53.06°, respectively. Essentially the same results were obtained using either the MM2 or DREIDING force fields. Calculations were implemented in the molecular mechanics program BIOGRAF.

that this orientation of the disaccharide rings was the only one that allowed the fatty acid chains to be parallel and so attain the closest packed configuration. These conditions, therefore, constituted a unique set of necessary and sufficient conditions which, if demonstrated practically, would lead to the correct three-dimensional structure of diphosphoryl lipid A.

The conformational requirements of the proposed structure could easily be verified by NMR spectroscopy. Lipopolysaccharides and lipid A molecules do not ordinarily give well-resolved NMR spectra. This was facilitated, however, by the use of a new solvent system that gives well-resolved spectra for many different classes of lipid molecules (Wang & Hollingsworth, 1995). A combination of homo- and hetero-two-dimensional NMR experiments were performed in order to allow the assignments of the signals for the carbohydrate protons. The signal for H-1 of the proximal glucosamine residue was readily assignable from the 500 MHz proton spectrum (Figure 4A). It appeared at 5.34 ppm as a doublet of doublets (J = 7.5 and 3.0 Hz) split by both H-2 and the phosphorus atom in the phosphate group. This assignment could readily be confirmed by a two-dimensional $^1H/^{31}P$ heteronuclear multiquantum coherence (HMQC) experiment which also indicated the identity of H-4 of the distal glucosamine residue (H-4′) which is also phosphorylated (see inset to Figure 4A). The next obvious assignments were the signals for the two C-3 protons. These appeared in the proton spectrum in the region of 4.9−5.1 ppm. This relatively downfield location was to be expected since the carbon atoms to which they are attached also bear electron-withdrawing acyloxy groups. Confirmation of these assignments and assignment of the other ring resonances as well as critical fatty acid resonances were obtained from two-dimensional double-quantum-filtered *J*-correlated spectroscopy (DQF-COSY) (Figure 4B) and total correlated spec-

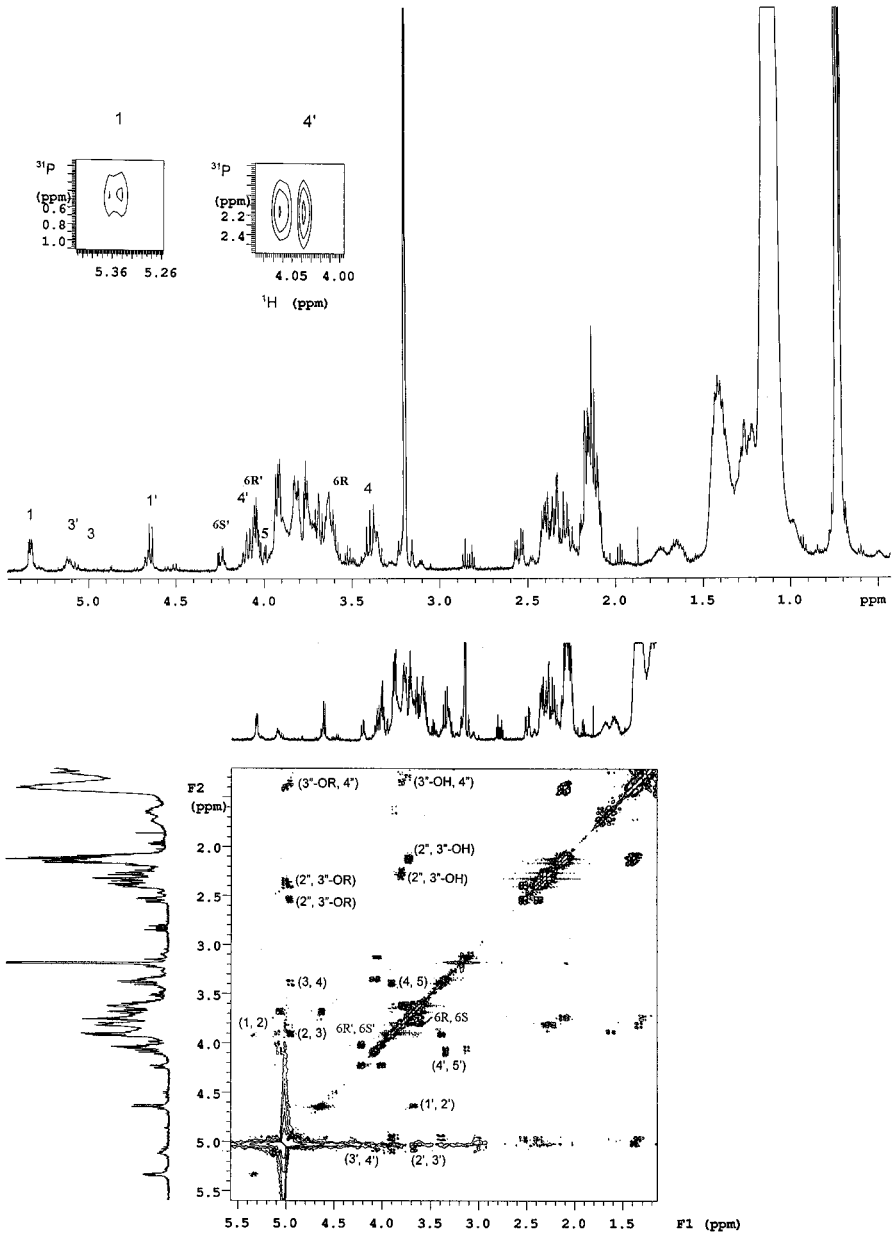

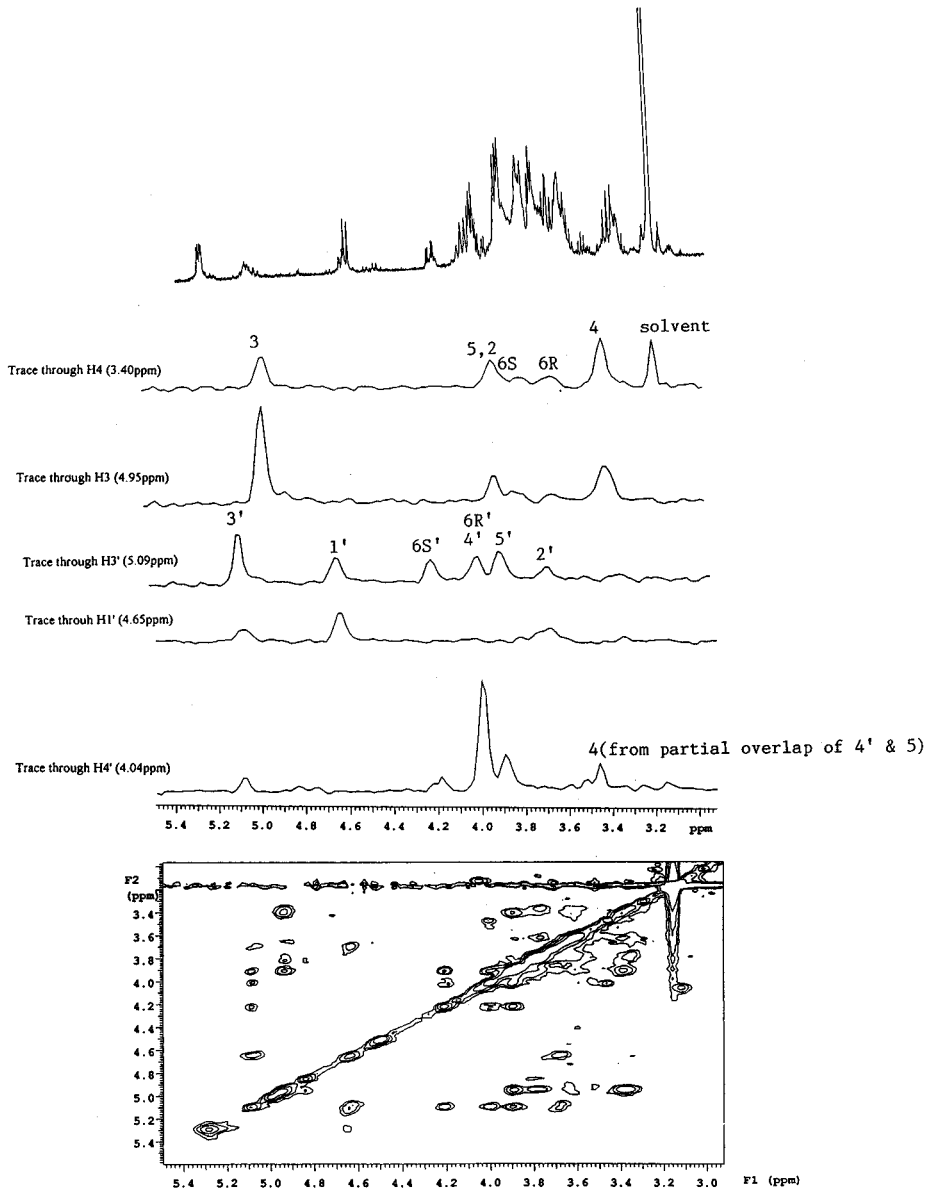

FIGURE 4: (A, top left) 500 MHz ^{1}H NMR spectrum of lipid A in 1:1:2:10 pyridine-d_5/37% DCl in D_2O/CD_3OD/CD_3Cl. The HOD line at 5.0 ppm was suppressed by presaturation. The insets show partial ^{1}H/^{31}P HMQC spectra. Note the correlations to the anomeric proton of the proximal ring residue (H-1) and to H-4′. (B, bottom left) DQF-COSY spectrum of lipid A. Cross peaks are labeled so that the unprimed numbers refer to the proximal glucosamine ring, the primed numbers refer to the distal ring, and the double primed numbers refer to the fatty acid chains. 3″-OH refers to the 3 position of a fatty acyl chain in which the hydroxyl group is free, and 3″-OR refers to one bearing an acyloxy substituent. (C, right) A partial TOCSY spectrum showing the connected spin systems of the two glucosamine rings. Traces through key protons are displayed above.

Table 1: Proton NMR Assignments for Carbohydrate Ring Protons[a]

	1	2	3	4	5	6(S,R)
H	5.34	3.89	4.95	3.40	3.99	3.77, 3.62
H′	4.65	3.68	5.09	4.04	3.88	4.22, 4.01

[a] H refers to proximal and H′ to distal ring resonances.

troscopy (TOCSY) experiments (Figure 4C). A complete analysis of the spin systems for the two ring systems with 1-D traces confirming the connectivities is given in Figure 4C, and the chemical shifts of the various protons are given in Table 1. One critical interpretation of the spectra was the stereospecific assignment of H-6R and H-6S of the proximal glucosamine ring. This was initially based partially on the fact that H-6S usually appears downfield of H-6R in glucosides and also, based on the model, H-6S must be close to the plane of the ring of both glucosamine residues and should be deshielded. The conformation indicated by the NOE results (see later) gave a more reliable indication which was still, however, in accord. The chemical shifts and coupling constants of the ring protons were all consistent with the pyranose rings still being in the $^4C_1$ configuration (regular chair forms) thus satisfying the first condition. One noticeable feature, however, was that the signal for the C-4′ proton displayed a slightly smaller coupling ($J = 6.5$ Hz) to both of its neighbors (H-3′ and H-5′). This indicated that the distal region of this ring was more puckered probably to accommodate the four acyl groups at the 2′ and 3′ positions. Once the assignments were made, it was then possible to demonstrate that a substantial NOE did exist between the anomeric proton of the distal glucosamine residue and H-4, H-6R, and H-6S protons of the proximal residue as required by the model. It was also possible to demonstrate that the relative amplitudes of the various NOEs were consistent with the various internuclear distances. This information was obtained primarily from the NOE spectra measured with a 200 ms mixing time. Spectra were acquired at different mixing times primarily to address the potential problem of spin diffusion. From the quality of the proton spectra (primarily the line widths which were typically only a few hertz) it was clear that the molecules were freely tumbling and that both the spin−lattice and spin−spin relaxation times were comparatively long for a medium-sized biomolecule. This would mean that the rotational correlation time (τ_c) would be short and the rate of NOE buildup (which for mixing times much smaller than the spin diffusion limit is proportional to τ_c times the inverse sixth power of the internuclear separation between the two relaxing nuclei) would be slow. If the mixing time is incremented, for the shorter mixing times at which cross peaks appear, one can then use the absolute amplitudes of the cross peaks as a measure of the rate of buildup and a direct measure of internuclear distance. The first substantial NOE buildup appeared at 200 ms. This is an ideal situation since it is much shorter than the spin−lattice relaxation time and the time limit at which spin diffusion should set in. A typical mixing time for a biomolecule of comparable size, say, for instance, a small oligonucleotide 10-mer duplex, is 350 ms (Feignon et al., 1979, 1983). The NOE spectrum at 200 ms mixing time (Figure 5) contained cross peaks corresponding to interactions between H-1 of the distal glucosamine residue and H-4, H-6R, and H-6S of the proximal residue. The expected relative NOE intensities were 1:0.33:0.044, respectively (normalized to the H-1′−H-4 NOE), based on the internuclear distances measured from the model. The primary assumption here was that there is no rotation about the interglycosidic bond by virtue of the acyl chain interactions and the amphiphilic nature of the molecules and hence no need to account for statistical sampling and weighting of populations on the values. This calculation also assumed no internal motion giving rise to preferential relaxation rates between any particular spin pair or pairs. The measured relative cross peak intensities were 1:0.45:0.061, respectively, in good agreement with the calculated values. An important (though smaller than expected) NOE was obtained for the H-1′−H-5′ interaction. This was again consistent with the idea that the distal glucosamine residue was slightly deformed, thus increasing the distance between H-1′ and the H-3′ and H-5′ diaxial neighbors. The NOE cross peak to H-5′ had a relative intensity of 0.029. The one to H-3′ was suppressed since it appeared very close to the solvent line. No NOE to H-5 was observed. A substantial NOE was observed between H-4 and H-6. This helped to confirm the stereospecific assignment of H-6R and H-6S. The distance

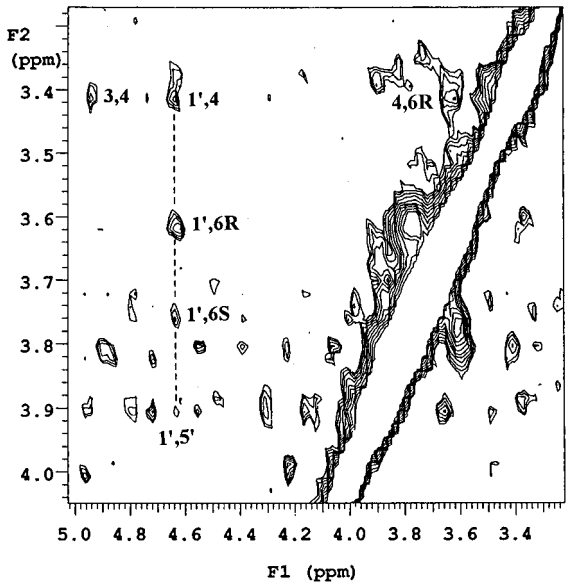

FIGURE 5: Partial NOE spectrum (200 ms mixing time) showing the various key interactions, especially those involving H-1′ and the protons on the proximal glucosamine ring. Note the strong NOE between H-4 and H-6R. The H-1′−H-5′ NOE is observed. The corresponding one to H-3′ is not observed because this signal is too close to the solvent line (HOD) which had to be suppressed.

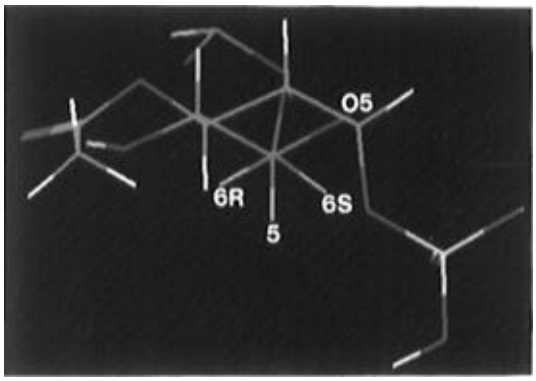

FIGURE 6: View along the C-5−C-6 bond of the reducing glucosamine residue showing the conformation of the alkoxymethyl group to be the *gg* rotamer. The distal glucosamine residue and the *N*-acyl group have been removed for clarity.

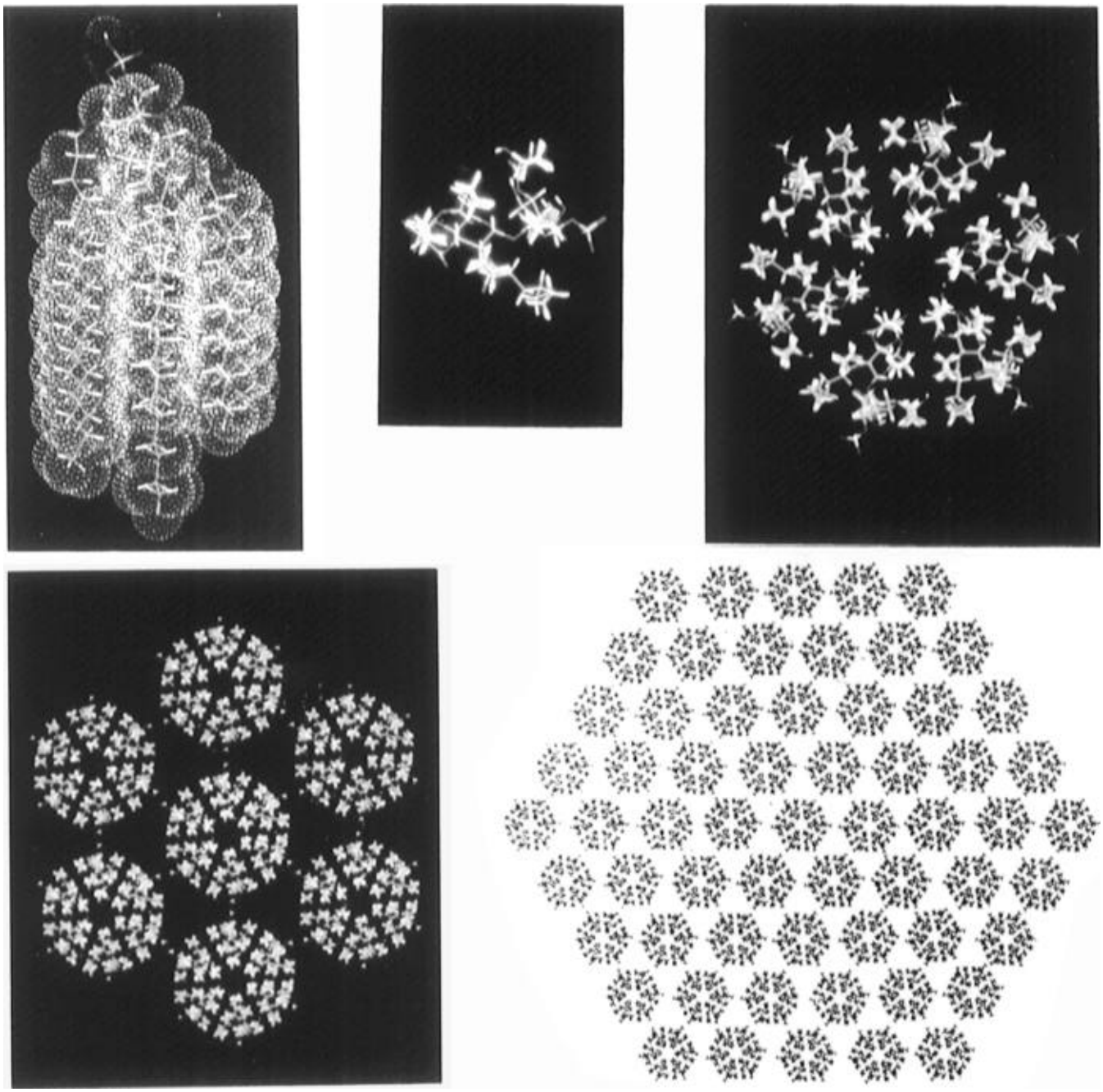

FIGURE 7: (A, top left) Vector model showing van der Waals surfaces of the calculated structure of the lipid A molecule shown in Figure 1. Note the extended alkyl chains. (B, top center) Structure seen from on top. Note the triangular cross section for the most efficient packing arrangement of the hydrocarbon chains. The 1-phosphate group is shown to the right. The leftmost alkyl chain is A in Figure 1. The topmost is E, the bottom is C, and the one closest to the 1-phosphate group is F. Of the two remaining chains, the topmost is B and the other D. (C, top right) A hexagonal array formed from six lipid A molecules with phosphate groups in the center bridged with calcium (white dots) ions. (D, bottom left) A larger array formed from seven of the units shown in (C). The units are held together by electrostatic bridges involving calcium and the six phosphate groups around each unit. (E, bottom right) A very large hexagonal array. There are other possible hexagonal arrangements of the basic structure.

between H-4 and H-6R in the proposed structure is 3.28 Å. This is less than the H-1′−H-6S distance, and the cross peak intensity was, as expected, substantially higher. No NOE was observed between H-4 and H-6s. This is again consistent with the other findings since the expected separation of these two nuclei is 3.90 Å. The H-1′−H-5 distance is very similar (4.03 Å), and no NOE was observed for this interaction.

The final step was to establish the magnitude of the dihedral angles in question. This could be established by determining the magnitudes of the vicinal coupling constant between H-5 and H-6R and the one between H-5 and H-6S. These coupling constants could then be related to the dihedral angles between the bonds involving them by a Karplus-type relationship (Karplus, 1959) or a more recently described variant that is well parametrized for carbohydrates (Haasnoot et al., 1980; Bock & Duus, 1994). In this latter relationship, a correlation is made between the magnitudes of the coupling constants for the H-5−H-6 interactions and the value of the torsion angle ω. A signal for the H-6R proton was discernible in the proton spectrum (Figure 4A). This appeared quite close to another small spurious signal but the correct multiplicity was readily evident by examining the COSY cross peaks. The H-6R signal appeared as a doublet

with a large splitting of 12 Hz, a typical value for geminal protons. There was no other splitting indicating a coupling constant of less than 1 Hz to H-5. The H-6S component was obscured by other signals, but an estimate of its splitting by H-5 could be obtained from examining the COSY cross peaks and traces and by measuring the peak width of its signal from the TOCSY traces. The value thus obtained was ~3−4 Hz. A definitive value could be obtained from examining the splitting of the H-5 signal. This was reasonably well resolved and appeared as a doublet of doublets (J = 8 Hz + 3.5 Hz). The larger coupling was due to splitting with the neighboring *trans* C-4 proton (a triplet with 8 Hz coupling). There was only one other splitting and this was assigned to the H-6S interaction since it was already known that the H-6R splitting was not discernible.

The Haasnoot−DeLeeuw−Altona relationship was preferred for use in conformational analysis because it is based on a very comprehensive data base of known structures and is comparatively well parametrized. This relationship gives the value of the coupling constant for the two vicinal couplings as a function of the torsion angle ω. Hence, if the two coupling constants can be measured, the value of ω can be calculated or determined graphically. The converse is also true; if a value for ω can be proposed, the observed coupling for the H-6R−H-5 and H-6S−H-5 coupling constants can be confirmed. The general form of the relationship is given in eq 1. A graphical solution was used. In this

$$^3J(\mathrm{HH}) = P_1 \cos^2(\omega) + P_2 \cos(\omega) + P_3 + \sum_i \Delta\chi_i [P_4 + P_5 \cos^2(\xi_i \omega + P_6 |\Delta\chi_i|)] \quad (1)$$

relationship, P_1, P_2, P_3, P_4, P_5, and P_6 are constants and $\Delta\chi_i$ is the electronegativity of substituent i at the C-6 position minus the electronegativity of hydrogen. When a value of −53 is used for ω, the relationship gives values of <1 Hz and ~4 Hz (respectively) for these coupling constants, in very good agreement with the measured values. These values also indicate that the alkoxymethyl group adopts the *gg* conformation. This is also in excellent agreement with that seen in the model (Figure 6). This is the most stable conformation for the hydroxymethyl group of hexopyranosides with the *gluco* configuration.

The calculated structures (Figure 7) can easily form extended hexagonal structures by van der Waals interactions between their fatty acid chains and electrostatic interactions by magnesium or calcium/phosphate salt bridges. Such extended hexagonal arrays have several possible configurations based on the same starting lipid A structure. These and their relative energies have been explored by Monte Carlo simulations (Jung et al., 1996). The simple geometrical symmetry of the monomer unit was exploited in these analyses.

The results described here advance a clear molecular basis for the observed structure and periodicity of lipopolysaccharide and lipid A aggregates. Other computational studies have appeared in the past (Katowsky et al., 1991; Labischinski et al., 1985), but none have identified regular structural elements which explain the observed geometries of lipid A aggregates. These also rely exclusively on calculation and do not incorporate any information from physical measurements. The results shown here identify the origins of the forces and geometric attributes which make lipopolysaccharides the highly efficient, self-assembling systems that they are. The interchain forces for the alkyl groups were in agreement with those obtained using Salem's approximation (Salem, 1962). These forces amounted to ~70 kcal/mol for a single isolated lipid A molecule. This is the value expected from Salem's approximation if the interactions are summed over a nearest and six next-nearest neighboring chains. These results should provide a firm molecular basis for rationalizing the effects of lipopolysaccharides on the dynamics and organization of membrane lipids as well as a structural basis for understanding the interaction between lipopolysaccharides and lipopolysaccharide binding molecules. It should be noted that the solvent system in which these NMR measurements were made was designed to reduce the intermolecular interactions between lipid A molecules but not to disturb the conformations of individual lipid molecules. This is a reasonable outcome for the use of such a solvent since one of the greatest contributions to the conformation of the lipid A molecule is the large number of short-ranged van der Waals interactions between the methylene groups of the six hydrocarbon chains. It is difficult for these to be offset by solvation of the chains by a solvent containing a large proportion of polar components such as methanol and HCl. It is reasonable, however, that any metal ions bridging phosphate groups between lipid A molecules should be replaced by the bulky and very abundant pyridinium group. This should break down inter-lipid interactions but not alter the conformations of individual lipid molecules appreciably since the charged groups do not interact in an intramolecular fashion.

REFERENCES

Bax, A., & Subramanian, S. (1986) *J. Magn. Reson. 67*, 565−569.

Bock, K., & Duus, J. O. (1994) *J. Carbohydr. Chem. 13*, 513−543.

Ernst, R. R., Bodenhansen, G., & Wokaun, A. (1987) *Principles of Nuclear Magnetic Resonance on One and Two Dimensions*, pp 431−440, Oxford University Press, Oxford.

Feignon, J., & Kearns, D. R. (1979) *Nucleic Acids Res. 6*, 2327−2337.

Feignon, J., Leupin, W., Denny, W. A., & Kearns, D. R. (1983) *Biochemistry 22*, 5943−5951.

Galanos, C., & Lüderitz, O. (1984) in *Handbook of Endotoxin* (Rietschel, E. T., Ed.) Vol. 1, pp 46−58, Elsevier, Amsterdam.

Gasteiger, J., & Marsili, M. (1980) *Tetrahedron 36*, 3219−3228.

Gery, I., & Waksman, B. J. (1972) *J. Exp. Med. 136*, 143−155.

Haasnoot, C. A., De Leeuw, F. A., & Altona, C. (1980) *Tetrahedron 36*, 2783−2792.

Jackson, S. K., James, P. E., Rowlands, C. C., & Evans, J. C. (1989) *Free Radical Res. Commun. 8*, 47−53.

Jackson, S. K., James, P. E., Rowlands, C. C., & Mile, B. (1992) *Biochim. Biophys. Acta 1135*, 165−170.

Jung, S., Min, D., & Hollingsworth, R. I. (1996) *J. Comput. Chem. 17*, 238−249.

Karplus, M. (1959) *J. Chem. Phys. 30*, 11−15.

Kastowsky, M., Gutberlet, T., & Bradaczek, H. (1993) *Eur. J. Biochem. 217*, 771−779.

Kato, N. (1993) *Micron 24*, 91−114.

Katowsky, M., Sabisch, A., Butberlet, T., & Brodaczek, H. (1991) *Eur. J. Biochem. 197*, 707−716.

Kim, K. I., Lill-Elghanian, & Hollingsworth, R. I. (1994) *Bioorg. Med. Chem. Lett. 4*, 1691−1696.

Labischinski, H., Barnickel, G., Brodaczek, H., Naumann, D., Rietschel, E. T., & Giebrecht, P. (1985) *J. Bacteriol. 162*, 9−20.

Larsen, N., Enelow, R., Simons, E., & Sullivan, R. (1985) *Biochim. Biophys. Acta 815*, 1−8.

Liljefors, T., Tai, J. C., Li, S., & Allinger, S. N. (1987) *J. Comput. Chem. 8*, 1051−1056.

Mayo, S. L., Olafson, B. D., & Goddard, W. A. (1990) *J. Phys. Chem. 94*, 8897−8909.
Morrison, D. C., & Ryan, J. L. (1979) *Adv. Immunol. 28*, 293−341.
Myers, K. R., Truchot, A. T., Ward, J., Hudson, Y., & Ulrich, J. T. (1990) in *Cellular and Molecular Aspects of Endotoxin Reactions* (Nowotny, A., Spitzer, J. J., & Ziegler, E. J., Eds.) Vol. 1, pp 145−156, Elsevier, Amsterdam.
Nowotny, A. (1969) *Bacteriol. Rev. 33*, 72−88.
Price, R., & Jacobs, D. (1986) *Biochim. Biophys. Acta 859*, 26−32.
Raetz, C. R. (1993) *J. Bacteriol. 175*, 5745−5753.
Rietschel, E. T., Brade, L., Holst, O., Kulsin, V. A., Linder, B., Morgan, A., Schade, U. F., Zähringer, U., & Brade, H. (1990) in *Cellular and Molecular Aspects of Endotoxin Reactions* (Nowotny, A., Spitzer, J. J., & Ziegler, E. J., Eds.) Vol. 1, pp 15−32, Elsevier, Amsterdam.
Salem, L. (1962) *Can. J. Biochem. Physiol. 40*, 1287−1298.
Schechmeister, I. L., Bond, V. P., & Swift, M. N. (1952) *J. Immunol. 68*, 87−93.
Shands, J. W. (1971) in *Microbial Toxins* (Weinbaum, G., Kadis, S., & Ajl, S., Eds.) Vol. 4, pp 127−144, Academic Press, New York.
Shands, J. W., Graham, J. A., & Nath, K. (1967) *J. Mol. Biol. 25*, 15−21.
Turner, M., Chantry, D., Bochan, G., Barrett, M., & Feldmall, M. (1989) *J. Immunol. 143*, 3556−3561.
Wang, Y., & Hollingsworth, R. I. (1995) *Anal. Biochem. 225*, 242−251.
Wright, S. D., Ramos, R. A., Tobias, P. S., Ulevitch, R. J., & Mathison, J. C. (1990) *Science 249*, 1431−1433.

BI950645P